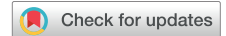# Novel Transcatheter Approach to Treat Primum Atrial Septal Defects

Check for updates

Gregory J. Condos, MD, James M. McCabe, MD, Denise C. Joffe, MD, and
Richard D. Sheu, MD, FASE, *Seattle, Washington*

INTRODUCTION

Atrial septal defects (ASDs) are among the most common congenital defects encountered in clinical practice. Secundum type defects account for roughly 80% of ASDs and when feasible are usually closed in the catheterization lab.[1] The next most common subtype is an ostium primum defect, or partial atrioventricular canal (AVC), which is a subtype of AVC defects.[2] Surgical closure is the standard of care because of the near universal presence of a mitral valve (MV) cleft with mitral regurgitation (MR), absent rims to secure a percutaneously delivered occluder device, and the proximity of the ASD to the atrioventricular valves (AVVs). Here we present a novel transcatheter treatment of a primum ASD guided by the use of advanced transesophageal echocardiography (TEE) techniques.

CASE PRESENTATION

A 56-year-old woman was referred to our institution with presumed Lutembacher's syndrome, which consists of an ASD and mitral stenosis (MS). The patient had experienced progressive heart failure over 2 years, culminating in a hospital admission at another institution for paroxysmal atrial fibrillation and pulmonary edema. Echocardiographic workup demonstrated MS (mean diastolic gradient of 11 mm Hg) from thickened MV leaflets with significant calcification at the leaflet tips, possibly from a rheumatic etiology, and a primum ASD with left-to-right shunt (Figure 1, Video 1). Right atrial (RA) and ventricular volumes were measured at 28 mL/m^2 by the modified biplane method and 46 mL/m^2 by three-dimensional (3D) echocardiography, respectively. The left atrial (LA) volume was moderately enlarged, measuring 43 mL/m^2 by the modified biplane method.

The patient adamantly declined open-heart surgery for fear of prolonged postoperative recovery and hospitalization in the COVID pandemic setting, despite multiple conversations from both the surgical and interventional team. The patient ultimately elected for balloon mitral valvuloplasty (BMV) and potential percutaneous primum ASD

VIDEO HIGHLIGHTS

Video 1: Three-dimensional TEE, midesophageal live view MPR display in the aortic valve long-axis (**A**, 148°) and 4-chamber (0°) view without (**B**) and with (**C**) color-flow Doppler, demonstrates the "hockey stick" anterior MV leaflet diastolic motion and the high-velocity flow through the primum ASD.

Video 2: Three-dimensional TEE using the single-beat focused imaging mode demonstrates the characteristics of common AVC defects, such as primum ASD, cleft in the anterior mitral leaflet (*arrow*), and anterior unwedging of the aortic annulus from the mitral and tricuspid annuli when viewed from the atrial perspective.

Video 3: (A) Live 3D TEE, volume-rendered display using the focused imaging mode with color-flow Doppler, demonstrates residual left-to-right shunt anteriorly to the ASD. **(B)** Two-dimensional TEE, midesophageal 4-chamber view, demonstrates appropriate inferior coverage of the ASD by the occluder device without impingement of MV. **(C)** Two-dimensional TEE with color-flow Doppler, midesophageal oblique long-axis (38°) view, demonstrates redirection of shunt flow to the left ventricle by the RA disk.

Video 4: (A) Two-dimensional TTE, apical 4-chamber view without (*left*) and with (*right*) color-flow Doppler, demonstrates redirection of shunt flow into the left ventricle. There is resolution of the interatrial shunting as demonstrated by agitated saline contrast injection during the Valsalva maneuver **(B)**.

View the video content online at www.cvcasejournal.com.

closure, even though the outcomes associated with this approach are largely unknown.

The patient was brought to the cardiac catheterization lab and placed under general anesthesia. Intraprocedural TEE was performed and confirmed the presence of moderate to severe MS (mean diastolic gradient of 9 mm Hg). Moderate MR with a vena contracta width of 0.32 cm was also appreciated. The primum ASD measured approximately 1.2 × 2.3 cm by 3D multiplanar reconstruction (MPR; Figure 2). The Qp:Qs shunt ratio was 3:1 by Fick.

Intraprocedural 3D TEE imaging showed a heavily calcified mitral apparatus with a cleft in the anterior leaflet. Additionally, the aortic valve was displaced anteriorly, unwedging it from the mitral and tricuspid valves. Although better appreciated on two-dimensional (2D) imaging, it was also noted that the AVV annuli were at the same level (Figure 3, Video 2).
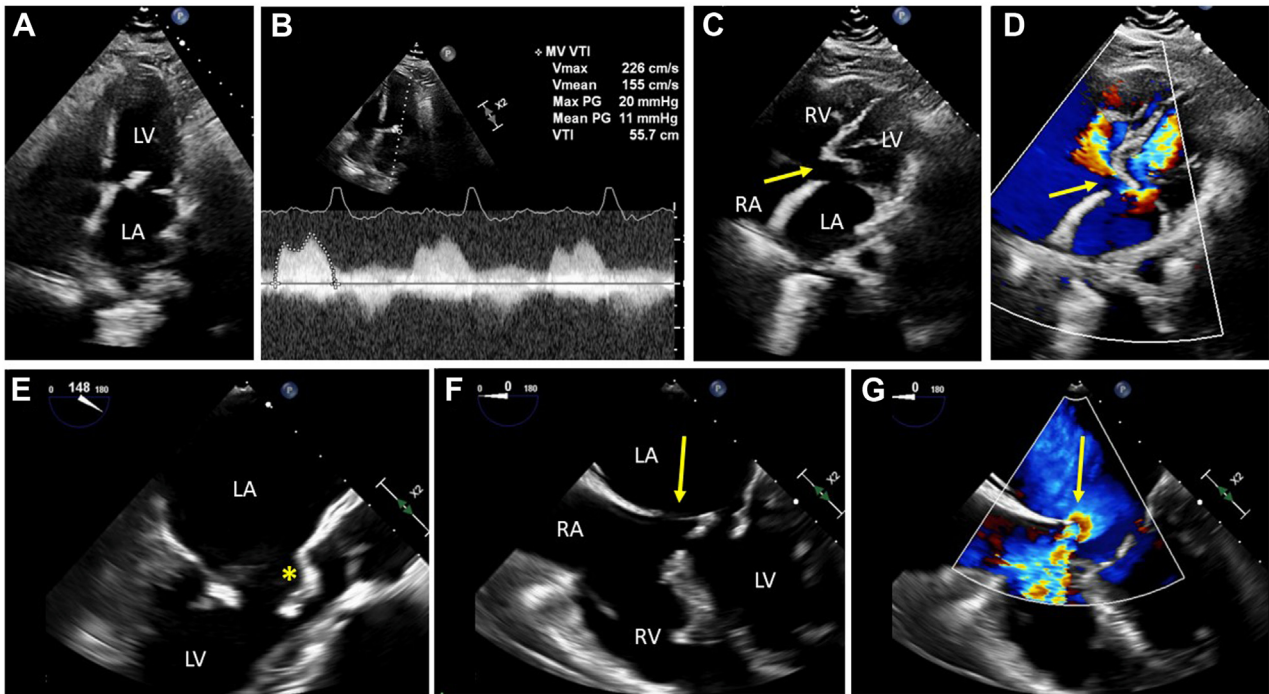
Figure 1 **(A)** Two-dimensional (2D) transthoracic echocardiogram (TTE), apical 4-chamber view during mid diastole, demonstrates diseased MV with **(B)** continuous-wave Doppler-determined elevated mean gradient. **(C, D)** Two-dimensional TTE, apical 4-chamber view without and with color flow Doppler, demonstrates an ASD (*yellow arrows*) with left-to-right shunt during mid diastole. **(E)** Two-dimensional TEE, midesophageal aortic valve long-axis view, during mid diastole demonstrates "hockey stick" anterior mitral leaflet (*asterisk*). **(F, G)** Two-dimensional TEE, midesophageal 4-chamber view without and with color-flow Doppler during mid diastole, demonstrates high-velocity flow through the primum ASD (*yellow arrows*). *LV*, Left ventricle; *RV*, right ventricle.

The combination of MV cleft, primum ASD, displaced aortic valve, and same AVV level was consistent with a partial AVC defect that was not definitively diagnosed preprocedure. The decision was made to abort the BMV due to both unfavorable mitral commissural anatomy and the degree of preexisting MR. Despite deficient anterior and inferior interatrial septum (IAS) tissue rim, the team elected to proceed with a novel percutaneous primum ASD closure approach as the risk of developing progressive right-sided heart failure outweighed the risk of attempting closure to reduce the shunt fraction.

A 12 French sheath was placed in the right femoral vein. A steerable guide catheter was advanced into the right atrium (RA) through the femoral sheath. Under live 3D MPR TEE guidance, the catheter was positioned approximately 3 to 5 mm above the ASD in the RA, with its tip abutting the IAS. A coronary guidewire was then passed through the catheter, electrified with a short burst of radiofrequency energy applied externally and punctured through the IAS into the left atrium (LA). This coronary wire was then exchanged for a stiffer wire, which was used as a rail for the dilator and device delivery sheath to advance safely into the LA. Through the delivery sheath, a 35 mm Amplatzer Cribriform occluder (Abbott), selected for its narrow waist (3 mm) and equally sized LA and RA disks, was deployed in typical fashion (Figure 4).
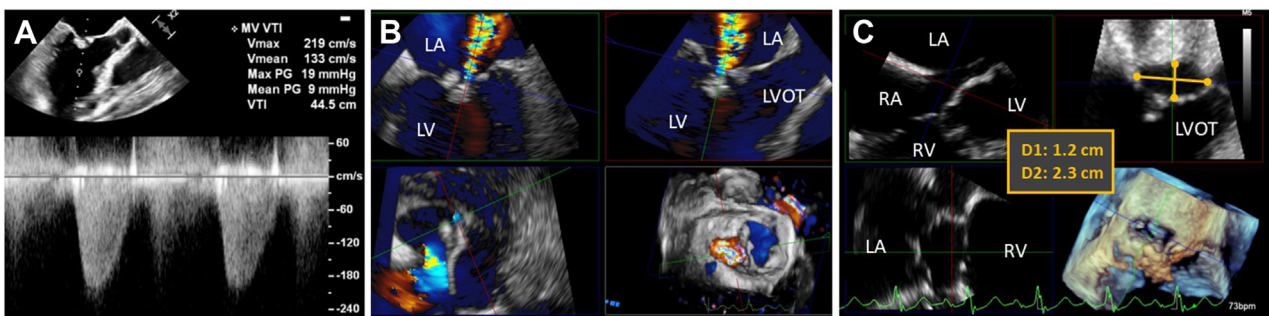

Figure 2 **(A)** Intraprocedural TEE confirmed stenosis pathology by continuous-wave Doppler through the MV. **(B)** Three-dimensional MPR with color-flow Doppler of the MR during midsystole with imaging planes transecting the regurgitant jet in the midesophageal bicommissural view (*top left*), midesophageal long-axis view (*top right*), and transgastric basal short-axis view (*bottom left*) and 3D volume-rendered display, left atrial perspective (*bottom right*). **(C)** Three-dimensional MPR of the primum ASD during mid diastole with the *top left image* showing the midesophageal 4-chamber view and the *top right image* transecting the ASD in the short axis, allowing for accurate dimension measurements.
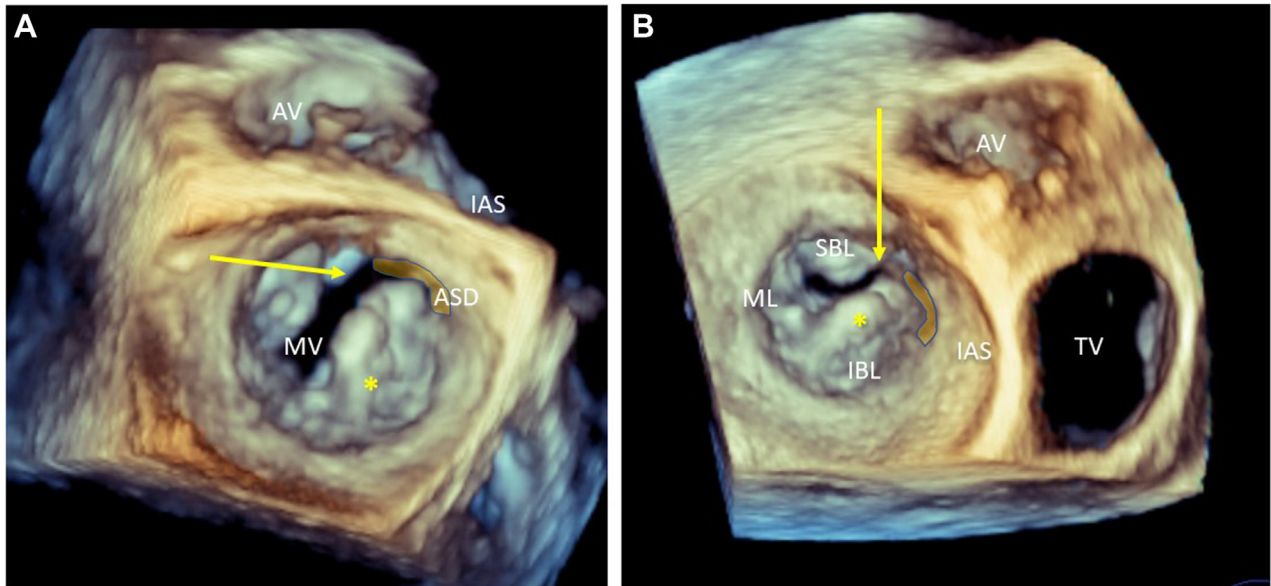
Figure 3 (A) Three-dimensional TEE, en face view of the MV using single-beat 3D focused imaging mode during mid diastole demonstrates primum ASD (*shaded area*) and anterior mitral leaflet cleft (*yellow arrow*). The *asterisk* indicates the calcium shelf above mitral leaflets. **(B)** Multibeat 3D large volume acquisition of the MV en face and surrounding structures during diastole demonstrates anterior unwedging of the aortic annulus from the mitral and tricuspid annuli. *AV*, Aortic valve; *IBL*, inferior bridging leaflet; *ML*, mural leaflet; *SBL*, superior bridging leaflet; *TV*, tricuspid valve.

The overhanging inferior rim of the occluder resulted in significant reduction in flow across the ASD without any negative interaction with the function of the AVVs. Preprocedural LA-to-RA flow during diastole had been reduced significantly with residual flow fortuitously directed toward the left ventricle by the RA occluder disk (Figure 5). Importantly, prior to release of the device, the mean gradient through the MV was unchanged at 9 mm Hg (Figure 5, Video 3).

The patient's electrocardiogram on postprocedural day 1 showed normal sinus rhythm with first-degree atrioventricular heart block and intraventricular conduction delay, unchanged from preprocedural findings (Figure 6). Follow-up TTE 1 month later confirmed resolution of interatrial shunting and no change in the MV inflow gradient (Figure 7, Video 4).

DISCUSSION

Lutembacher's syndrome has various definitions in the literature but at its core describes a syndrome of combined MS and an ASD. Because pressure in the LA can be offloaded by the ASD (depending on the size of the defect), patients can tolerate progressive MS longer than expected, at the expense of increasing left-to-right shunt and pulmonary overcirculation. Eventually this can lead to right-sided volume overload and failure; thus correction is recommended once the syndrome is recognized. Worldwide, most cases result from rheumatic heart disease in combination with a secundum ASD, although the syndrome has been described with any ASD and any etiology of congenital or acquired MS.[3] While rheumatic
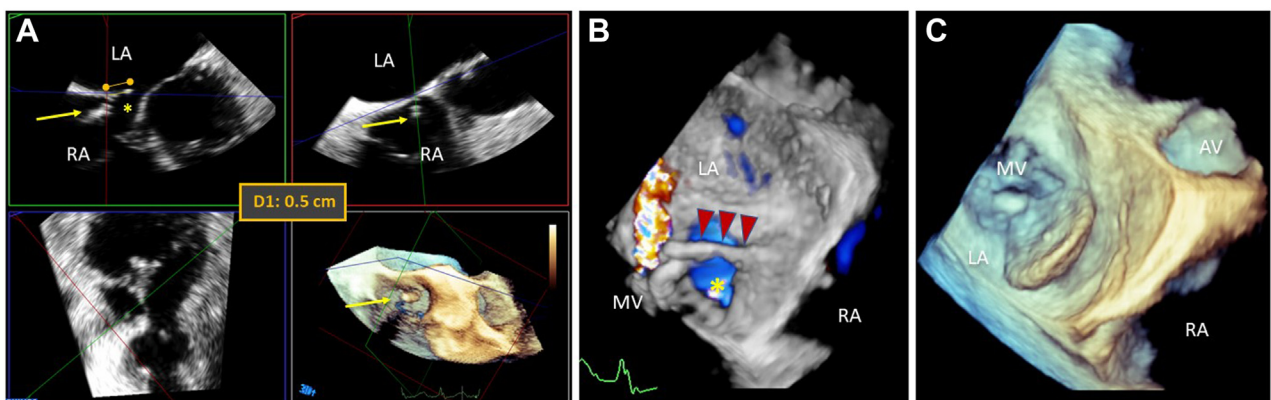

Figure 4 (A) Live 3D TEE with MPR using focused imaging mode during mid diastole showing steerable catheter (*yellow arrow*) approximately 5 mm superior to the ASD (*) in the midesophageal 4-chamber view (*top left*), interatrial septal view (*top right*), MPR en face view (*bottom left*), and volume-rendered display (*bottom right*). **(B)** Live 3D image acquired with focused imaging mode during midsystole from LA perspective showing the appropriate location of the device delivery sheath (*red arrowheads*) after transseptal puncture and **(C)** final device positioning in relation to the MV.
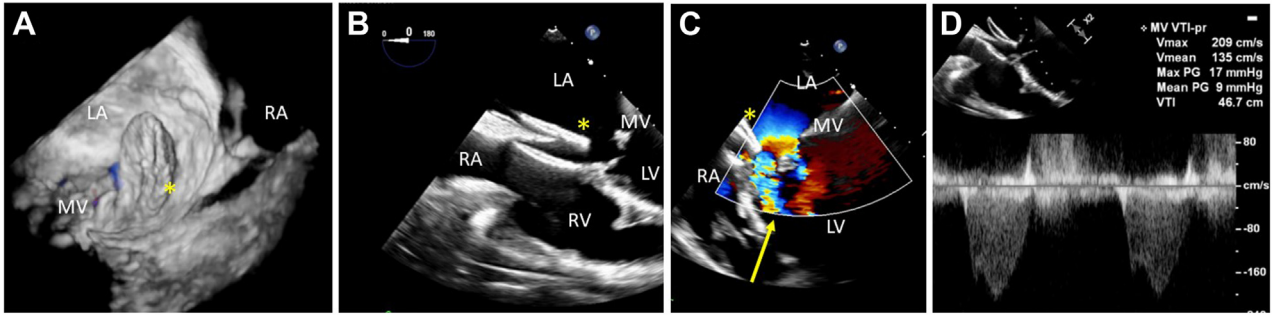
Figure 5 **(A)** Live 3D TEE acquired by focused imaging mode with color-flow Doppler during mid diastole demonstrates trace residual left-to-right shunt anteriorly to the ASD. **(B)** Two-dimensional TEE in the midesophageal 4-chamber view during mid diastole demonstrates inferior coverage of ASD by occluder device without impingement of the MV and **(C)** redirection of shunt flow to the left ventricle by the RA disk (*yellow arrow*) by color-flow Doppler. **(D)** Continuous-wave Doppler through the MV showing unchanged diastolic gradient after occlusion of the ASD. *Atrial septal occluder.
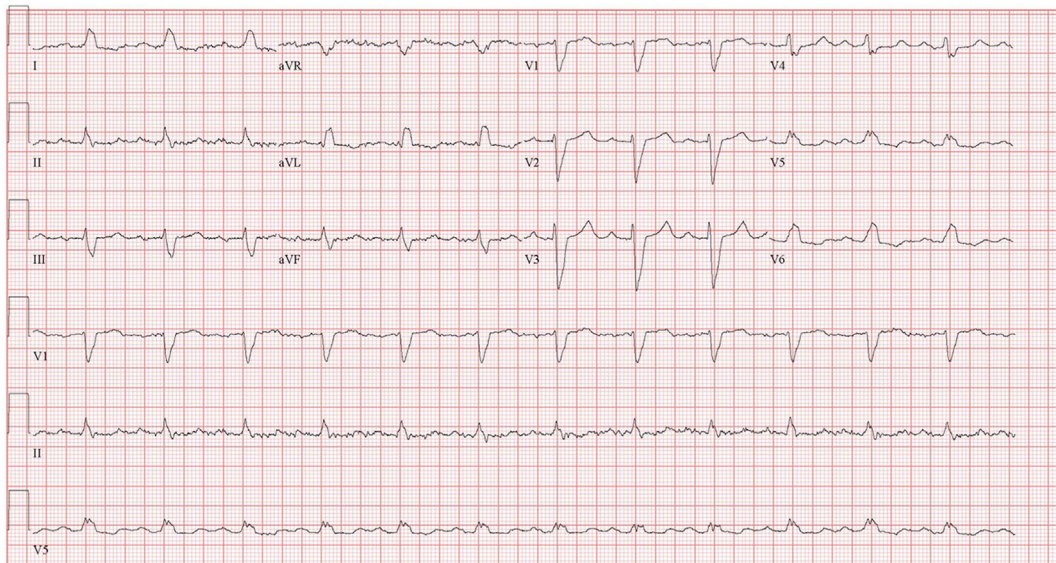

Figure 6 Postprocedural 12-lead electrocardiogram demonstrates normal sinus rhythm with first-degree atrioventricular heart block and intraventricular conduction delay.

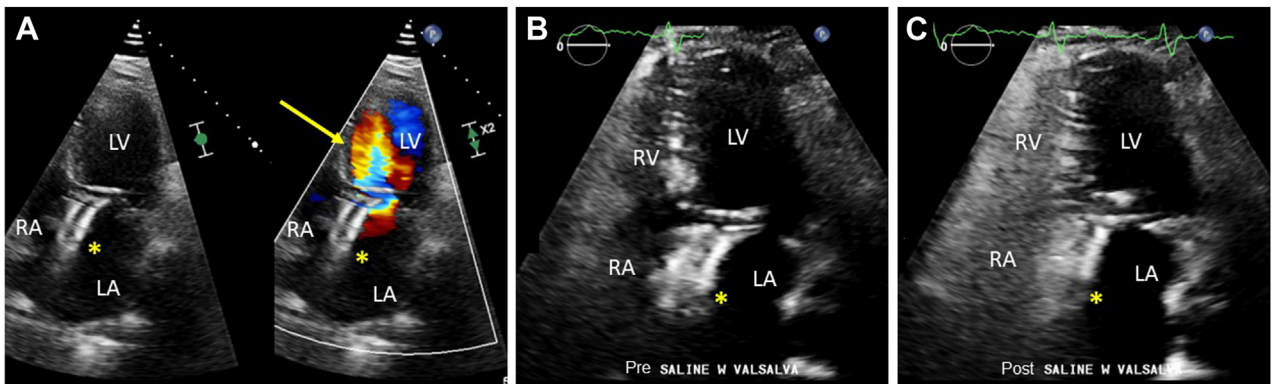**Figure 7** **(A)** Two-dimensional TTE, apical 4-chamber view without (*left*) and with (*right*) color-flow Doppler during mid diastole, demonstrates redirection of shunt flow (*yellow arrow*) into the left ventricle. The septal occluder device is seen as parallel echogenic lines (*) **(B)**, and there is resolution of the interatrial shunting as demonstrated by agitated saline contrast injection **(C)**.

heart disease was suspected in this case, intraprocedural TEE demonstrated the MV abnormality was more consistent with a degenerative partial AVC defect. However, rheumatic and congenital heart diseases are not mutually exclusive and could both be present in our patient. Nevertheless, the degree of MR precluded the use of BMV as a therapy for our patient's MS.

The spectrum of AVC defects results from varying degrees of failure of the development of the endocardial cushions and can range from isolated primum ASD to complete AVC defect, characterized by primum ASD, deficiency of ventricular septum, and single common AVV annulus.[4] The presence of a large oval-shaped AVV annulus results in anterior and superior displacement of the aortic valve annulus, which in turn elongates the left ventricular outflow tract (LVOT) into the "gooseneck deformity" frequently described in this particular congenital heart disease. Along with abnormally attached chordal structures from left-sided superior bridging leaflet to the ventricular septum, risk for LVOT obstruction is elevated compared with the general population. Another feature of AVC defects is the additional zone of apposition or cleft between the superior and inferior bridging mitral leaflets, which tend to result primarily in regurgitant valves.[5] While most patients present in infancy, patients with less severe forms of AVC defects can present in adulthood. Less commonly, degenerative changes to the AVV could change a regurgitant valve over time into a predominantly stenotic one, as in our patient. Heavy calcifications of the bridging leaflets and restriction from aberrantly attached chordae could mimic the diastolic doming appearance frequently associated with rheumatic disease.

Symptomatic primum ASDs carry a 1B recommendation for surgical closure in the most recent American College of Cardiology/American Heart Association guidelines for the management of adult congenital heart disease.[6] Surgical outcomes have been excellent, with low mortality and morbidity rates including cerebrovascular accidents, supraventricular arrhythmia, postpericardiotomy syndrome, and so on.[7] Percutaneous closure is not recommended due to deficient anterior and inferior septal rim for the device to be effectively secured. Moreover, the device could potentially interact and disrupt the AVVs and conduction system.

This case highlights a unique strategy for percutaneous closure of a primum ASD. By placing the device not through the ASD but through the IAS, we not only mitigated the risk of device embolism but also shifted the occluder disks away from the AVVs. This creative technique is made possible because of our increased familiarity and experience with radiofrequency-assisted tissue traversal in transcatheter interventions. By focusing electroenergy to the tip of a guidewire, precise perforation of the IAS could be achieved without applying excessive tension on the tissue. This technique is shown to be simple and safe in several anatomically challenging patients.[8] In our case, we uniquely employed electroenergy on the superior rim of a primum ASD to facilitate puncturing of the highly mobile IAS. Advanced intraprocedural TEE techniques such as real-time 3D MPR are important to accurately guide the steerable catheter to its ideal target on the IAS. Adjusting 3D MPR imaging planes to transect the steerable catheter in real time, the catheter position, engagement force, and approach angle to the IAS can be carefully assessed. Furthermore, the distance between the transeptal site and the tissue edge of the ASD can be measured as demonstrated in this case. Fortunately, the MV inflow gradient did not increase after ASD closure, although the patient continues to experience symptoms from severe MS. Since the location for primum ASD closure does not preclude future transseptal access, the patient can be considered for enrollment in trials of dedicated devices for transcath-

eter MV replacement. However, her innate risk for LVOT obstruction, associated with the AVC defect, may be the limiting factor and require other innovative solutions. It is important to recognize that the long-term outcome and durability of this transcatheter approach to primum ASD closure is currently unknown. Late complications from transcatheter ASD closure, including but not limited to device-related thrombosis, erosion, and infective endocarditis, will need to be closely monitored.

CONCLUSION

We report a successful transcatheter treatment of a primum ASD in a patient who refused surgical treatment. By puncturing the IAS superior to the primum ASD facilitated by radiofrequency energy, we were able to achieve percutaneous closure while mitigating risk of both device embolization and device interaction with the AVVs. With proper ASD sizing, device selection, and positioning, risk of residual shunt after device deployment was minimized.

ETHICS STATEMENT

The authors declare that the work described has been carried out in accordance with The Code of Ethics of the World Medical Association (Declaration of Helsinki) for experiments involving humans.

CONSENT STATEMENT

Complete written informed consent was obtained from the patient (or appropriate parent, guardian, or power of attorney) for the publication of this study and accompanying images.

FUNDING STATEMENT

DISCLOSURE STATEMENT

The authors report no conflicts of interest.

SUPPLEMENTARY DATA

Supplementary data related to this article can be found at https://doi.org/10.1016/j.case.2023.12.002.

REFERENCES

1. Moore J, Hegde S, El-Said H, Beekman R III, Benson L, Bergersen L, et al., ACC IMPACT Steering Committee. Transcatheter device closure of atrial septal defects: a safety review. JACC Cardiovasc Interv 2013;6:433-42.
2. Celermajer DS. Atrial septal defects: even simple congenital heart diseases can be complicated. Eur Heart J 2018;39:999-1001.
3. Mahajan K, Oliver TI. Lutembacher syndrome. 2023 mar 6. In: StatPearls [Internet]. Treasure Island (FL): StatPearls Publishing; 2023.
4. Calabrò R, Limongelli G. Complete atrioventricular canal. Orphanet J Rare Dis 2006;1:8.

5. Gatzoulis M, Webb G, Daubeney P. Atrioventricular septal defect. In: Diagnosis and Management of Adult Congenital Heart Disease. Elsevier Health Sciences; 2010.
6. Stout KK, Daniels CJ, Aboulhosn JA, Bozkurt B, Broberg CS, Colman JM, et al. 2018 AHA/ACC guideline for the management of adults with congenital heart disease: Executive summary: a report of the American College of Cardiology/American heart association Task force on clinical Practice guidelines. J Am Coll Cardiol 2019;73:1494-563.
7. Chowdhury UK, Airan B, Malhotra A, Bisoi AK, Kalaivani M, Govindappa RM, et al. Specific issues after surgical repair of partial atrioventricular septal defect: actuarial survival, freedom from reoperation, fate of the left atrioventricular valve, prevalence of left ventricular outflow tract obstruction, and other events. J Thorac Cardiovasc Surg 2009;137:548-5552.
8. Khan JM, Rogers T, Eng MH, Lederman RJ, Greenbaum AB, et al. Guidewire electrosurgery-assisted trans-septal puncture. Catheter Cardiovasc Interv 2018;91:1164-70.